Proc. Natl. Acad. Sci. USA
Vol. 96, pp. 3634–3639, March 1999
Biochemistry

Uncoupling of transfer of the presequence and unfolding of the mature domain in precursor translocation across the mitochondrial outer membrane

TAKASHI KANAMORI*, SHUH-ICHI NISHIKAWA*, MASATO NAKAI*†, INJAE SHIN‡§, PETER G. SCHULTZ‡¶, AND TOSHIYA ENDO*¶

*Department of Chemistry, Faculty of Science, Nagoya University, Nagoya 464-8602, Japan; and ‡Howard Hughes Medical Institute, Department of Chemistry, University of California, Berkeley, CA 94720

Contributed by Peter G. Schultz, January 28, 1999

ABSTRACT **Translocation of mitochondrial precursor proteins across the mitochondrial outer membrane is facilitated by the translocase of the outer membrane (TOM) complex. By using site-specific photocrosslinking, we have mapped interactions between TOM proteins and a mitochondrial precursor protein arrested at two distinct stages, stage A (accumulated at 0°C) and stage B (accumulated at 30°C), in the translocation across the outer membrane at high resolution not achieved previously. Although the stage A and stage B intermediates were assigned previously to the forms bound to the cis site and the trans site of the TOM complex, respectively, the results of crosslinking indicate that the presequence of the intermediates at both stage A and stage B is already on the trans side of the outer membrane. The mature domain is unfolded and bound to Tom40 at stage B whereas it remains folded at stage A. After dissociation from the TOM complex, translocation of the stage B intermediate, but not of the stage A intermediate, across the inner membrane was promoted by the intermembrane-space domain of Tom22. We propose a new model for protein translocation across the outer membrane, where translocation of the presequence and unfolding of the mature domain are not necessarily coupled.**

Most mitochondrial proteins are encoded by the nuclear genome, synthesized in the cytosol as precursor proteins, and imported into mitochondria. The mitochondrial targeting signal is, in many cases, contained in the presequence, which is an N-terminal extension of the precursor protein and cleaved off by matrix-processing peptidase (MPP) after import into the matrix (1). The presequence has a potential to form a positively charged amphiphilic helix, which represents the mitochondrial targeting signal. Translocation of mitochondrial precursor proteins across the mitochondrial membranes requires coordinated actions of translocation machineries in the outer and the inner membranes, TOM (translocase of the outer membrane) and TIM (translocase of the inner membrane) complexes, respectively (2–5).

In the past, many components of the TOM and TIM complexes have been identified. The TOM complex of yeast *Saccharomyces cerevisiae* consists of at least eight TOM proteins: Tom70, Tom37, Tom20, Tom22, Tom40, Tom5, Tom6, and Tom7. Among these TOM proteins, only Tom40 and Tom22 are essential proteins for cell growth (6–8). Tom40 is an integral membrane protein and forms a protein-conducting channel in the outer membrane (9, 10). Tom22 is anchored to the outer membrane by a central trans-membrane segment. The N-terminal cytosolic domain is highly acidic, and the C-terminal intermembrane space (IMS) domain contains some acidic residues, too. The roles of the cytosolic domain and the IMS domain of Tom22 in protein import have been a matter of debate (11–15).

The question, what drives protein translocation across the outer and inner membranes in mitochondria, is one of the key issues in the protein import into mitochondria. The outer membrane lacks any transmembrane electrochemical potential or ATP-driven chaperones on the trans side of the membrane. A model was proposed in which the mitochondrial outer membrane has two binding sites for the presequence, the cis site on the cytosolic side and the trans site on the IMS side of the outer membrane (16). The transfer of the presequence from the cis site to the trans site was suggested to be coupled with unfolding of the mature domain and to drive vectorial translocation of the precursor protein across the outer membrane. Characterization has been made for the translocation intermediates bound to the cis or the trans site as well as for possible components constituting the cis and the trans sites (14, 16–18).

To reveal a sequence of interactions between precursor proteins and each of the TOM and TIM components, we have been taking an approach of site-specific photocrosslinking aided by the suppressor tRNA method (19). We used pSu9-DHFR, a fusion protein between the presequence of subunit 9 of the F_0-ATPase and mouse dihydrofolate reductase (DHFR), as a model mitochondrial precursor protein to generate two distinct translocation intermediates at stage A and stage B, which meet the characteristics of the cis-site bound form and the trans-site bound form, respectively, and to analyze their interactions with TOM proteins. Unexpectedly, the results of site-specific photocrosslinking revealed that the presequence of pSu9-DHFR at both stages A and B is on the trans side of the outer membrane and that the mature DHFR domain of pSu9-DHFR is unfolded and trapped by Tom40 at stage B but not at stage A. Unfolding of the mature DHFR domain thus is not a prerequisite for the presequence to cross the outer membrane. Dissociation of both stage A and stage B intermediates from the TOM complex does not require the IMS domain of Tom22 whereas subsequent translocation of the stage B intermediate, but not of the stage A intermediate, across the inner membrane was promoted by the IMS domain

The publication costs of this article were defrayed in part by page charge payment. This article must therefore be hereby marked "*advertisement*" in accordance with 18 U.S.C. §1734 solely to indicate this fact.

PNAS is available online at www.pnas.org.

Abbreviations: MPP, matrix-processing peptidase; DHFR, mouse dihydrofolate reductase; pSu9-DHFR, a fusion protein between the presequence of subunit 9 of the F_0-ATPase and DHFR; CCCP, carbonyl cyanide *m*-chlorophenylhydrazone; BPA, 2-amino-5-(*p*-benzoylphenyl)pentanoic acid; MSC, 2-mesitylenesulfonyl chloride; IMS, mitochondrial intermembrane space; ΔC-Tom22, mutant Tom22 that lacks its C-terminal IMS domain; TOM, translocase of the outer membrane; TIM, translocase of the inner membrane.

†Present address: The Institute for Protein Research, Osaka University, Suita 565-0871, Japan.
§Present address: Department of Chemistry, Yonsei University, Seoul 120-749, Korea.
¶To whom reprint requests should be addressed.

of Tom22. The results will be discussed in the framework of a new model for protein translocation across the outer membrane, in which translocation of the presequence and unfolding of the mature domain are not necessarily coupled.

MATERIALS AND METHODS

Plasmids. The gene for the precursor of subunit 9 of *Neurospora crassa* F_0-ATPase was cloned into the *Sal*I site of pUC118. The resulting plasmid was used as template for PCR by using primers 5′-caggaaacagctatgac-3′ and 5′-cgcctcgaggagtaggcgcgcttctg-3′ to generate a DNA fragment encoding the presequence (the first 69 residues) of F_0-ATPase subunit 9. The amplified 0.3-kb fragment was digested with *Eco*RI and *Xho*I and ligated into the *Eco*RI and *Xho*I sites of pEH18 (20) to generate a DNA segment encoding pSu9-DHFR, in which a linker peptide, RSGI, was inserted between the presequence of F_0-ATPase subunit 9 and mouse DHFR. The segment for pSu9-DHFR was subcloned into pGEM-2 (Promega), and the resultant plasmid was named pSD(69). The codons for residues 6, 11, 15, 16, 17, 18, 19, 20, 21, 22, 23, 24, 25, 26, 27, 28, and 29 in the presequence and residues 78, 88, 98, and 108 in the DHFR domain of pSu9-DHFR were replaced by a TAG codon according to the published procedure (21).

Binding and Import of pSu9-DHFR *in Vitro*. pSu9-DHFR was synthesized in rabbit reticulocyte lysate in the presence of [^{35}S]methionine. Mitochondria were isolated from the yeast strain D273–10B, strain MNMS-MAS17 (wild-type mitochondria), or strain MNMS-MAS17Δ120–152 [ΔC-Tom22 (mutant Tom22 that lacks its C-terminal IMS domain) mitochondria; ref. 12] as described by Daum *et al.* (22). Binding and chase experiments for pSu9-DHFR with isolated mitochondria were performed as follows. Mitochondria (0.5 mg protein/ml) were preincubated in binding buffer [10 mM MOPS/KOH, pH 7.2/250 mM sucrose/10 mM KCl/5 mM $MgCl_2$/2 mM methionine/10 μM carbonyl cyanide *m*-chlorophenylhydrazone (CCCP; Sigma)] for 3 min at 0°C to dissipate $\Delta\Psi$. Then, the mitochondria were incubated with radiolabeled pSu9-DHFR for 10 min at 0 or 30°C. The samples were diluted 5-fold with MSC buffer (10 mM MOPS/KOH, pH 7.2/250 mM sucrose/10 μM CCCP] containing appropriate concentrations of KCl and were incubated for 5 min at 0°C. The samples were divided into halves, and mitochondria were reisolated by centrifugation at 12, 000 $\times$ *g* for 10 min. One aliquot was resuspended with binding buffer and kept on ice (for binding). The other aliquot was resuspended with chase buffer [10 mM MOPS/KOH, pH 7.2/250 mM sucrose/10 mM KCl/5 mM $MgCl_2$/10 mM DTT/2% (wt/vol) BSA/2 mM ATP/2 mM KP_i/5 mM sodium malate/2 mM NADH] and incubated for 10 min at 30°C (for chase). The chase reaction was stopped by adding valinomycin to 10 μg/ml. All the samples were analyzed by SDS/PAGE and radioimaging with a Storm 860 image analyzer (Molecular Dynamics).

Photocrosslinking. An amino acid with a photoreactive benzophenone side chain, 2-amino-5-(*p*-benzoylphenyl)pentanoic acid (BPA), was introduced at various positions of pSu9-DHFR labeled with [^{35}S]methionine by the suppressor tRNA method as described previously (19). BPA bearing pSu9-DHFR was incubated with mitochondria that had been treated with CCCP for 10 min at 0 or 30°C. The samples were diluted 5-fold with 2-mesitylenesulfonyl chloride (MSC) buffer containing 10 mM KCl and incubated for 5 min at 0°C; then, the mitochondria were isolated by centrifugation. The mitochondrial pellets were suspended in the same buffer (to 0.5 mg mitochondrial protein/ml) and were UV-irradiated for 5 min on ice as described previously (19). Immunoprecipitation with antibodies raised against Tom40 and Tom22 was performed as described previously (19).

RESULTS AND DISCUSSION

Precursor Protein Is Accumulated at Different Stages of Translocation Across the Outer Membrane Under $-\Delta\Psi$ Condition. We have used pSu9-DHFR as a model precursor protein to analyze interactions between a precursor protein and components of the TOM complex upon its passage across the outer membrane. pSu9-DHFR appears to contain a mitochondrial targeting signal in residues 16–29 of the presequence, because a pSu9-DHFR derivative lacking residues 1–14 of the presequence is imported efficiently into isolated mitochondria *in vitro* (data not shown) and hydrophilic residues including basic amino acids and hydrophobic residues are well segregated on the two sides of the helical wheels for the region of residues 16–29.

pSu9-DHFR bound to the mitochondrial surface when incubated with isolated mitochondria that had been treated with CCCP, which abolishes the membrane potential across the inner membrane ($\Delta\Psi$) and prevents translocation across the inner membrane (Fig. 1). When bound to mitochondria at 0°C, the bound protein generated a protease-resistant DHFR domain after a treatment with proteinase K (Fig. 1, lanes 1–3), suggesting that the DHFR domain was folded and exposed to the cytosolic face. We call this stage "stage A." On the other hand, when bound to mitochondria at 30°C, the DHFR part of the bound fusion protein became highly sensitive to proteinase K digestion, suggesting that the DHFR moiety is already unfolded (Fig. 1, lanes 4–6). We call this stage "stage B." When bound to mitochondria in the presence of methotrexate and NADPH, ligands for the DHFR moiety, at 30°C, the bound fusion protein generated a protease-resistant DHFR domain after a proteinase K treatment (data not shown), suggesting that inhibition of unfolding of the DHFR part leads to accumulation of the fusion protein at stage A but not at stage B. Next, purified matrix-processing peptidase (MPP; ref. 22) was added to probe the accessibility of the MPP cleavage site between the presequence and the DHFR domain. The presequence of the fusion protein bound to mitochondria at 0°C was cleaved off efficiently by externally added MPP (Fig. 1, lanes 7–9). On the other hand, the efficiency of the presequence cleavage by MPP was much lower for the fusion protein bound to mitochondria at 30°C than that bound at 0°C (Fig. 1, lanes 10–12). This suggests that the MPP-processing

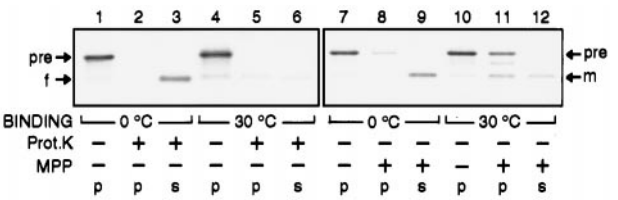

FIG. 1. The DHFR domain of pSu9-DHFR is unfolded at stage B but not at stage A on the mitochondrial surface. pSu9-DHFR was incubated with CCCP-treated mitochondria for 10 min at 0°C (lanes 1–3 and 7–9) or at 30°C (lanes 4–6 and 10–12). After 5-fold dilution with MSC buffer containing 10 mM KCl, 1 μM methotrexate, and 1 mM NADPH, the mitochondria were reisolated by centrifugation and were resuspended in the same buffer. The samples were divided into halves. For lanes 1–6, one aliquot was kept at 0°C (lanes 1 and 4) and the other was treated with 100 μg/ml proteinase K for 15 min at 0°C, which was inactivated by the subsequent addition of 1 mM phenylmethylsulfonyl fluoride (lanes 2, 3, 5, and 6). For lanes 7–12, one aliquot was kept at 0°C (lanes 7 and 10) and the other was treated with 2 μg/ml MPP and 1 mM $MnCl_2$ for 5 min at 30°C, and MPP was inactivated by the subsequent addition of 5 mM EDTA (lanes 8, 9, 11, and 12). The samples were centrifuged, and proteins in the pellet (p) and those in the supernatant (s), which were precipitated with trichloroacetic acid, were analyzed by SDS/PAGE. TEMP, temperature during the binding reaction; p, pellet; s, supernatant; pre and m, precursor and mature forms of pSu9-DHFR, respectively; f, proteinase K-resistant DHFR domain.

site in the fusion protein is exposed to the cytosolic face at stage A, but that it is somehow shielded from externally added MPP at stage B.

All of these results are consistent with the interpretation that pSu9-DHFR accumulated at stage A corresponds to the cis site bound form and the one at stage B to the trans site bound form (14, 16–18). It is interesting to note that a small but distinct amount of the mature DHFR fragment formed by MPP at stage B still was bound to mitochondria whereas that generated at stage A was completely released into the supernatant. Therefore, at stage B, not only the presequence but also the DHFR moiety of the fusion protein interacts stably with the TOM complex.

Relative Geometry Between the Presequence and the TOM Complex Does Not Differ Between Stage A and Stage B, but the Mature DHFR Domain Interacts with Tom40 More Strongly at Stage B than at Stage A. We introduced an amino acid with a photoreactive benzophenone, BPA, at various positions including both the presequence and the DHFR part of pSu9-DHFR. The introduction of BPA did not affect import or binding properties of pSu9-DHFR significantly (data not shown). The labeled fusion protein was incubated with CCCP-treated mitochondria at 0°C or at 30°C. The resultant mitochondria were diluted with washing buffer containing 10 mM KCl, reisolated by centrifugation, and subjected to UV irradiation for photocrosslinking. When introduced at residues 15, 20, and 27 in the presequence and at residue 108 in the DHFR part, BPA generated crosslinked products designated as X1–X7 in a manner that depended on light irradiation and positions (residues) of BPA (Fig. 2*A*). Proteins that were crosslinked to BPA were identified by solubilization of the mitochondria followed by immunoprecipitation with specific antibodies against the known components of the TOM complex. The crosslinking partner for X2 thus was assigned to Tom22 and those for X3–X7 were assigned to Tom40 (data not shown). A variation in the apparent molecular sizes of the crosslinked products involving Tom40 may reflect different configurations of the crosslinked products. The crosslinking partner for X1 (Fig. 2*A*) may be one of the small Tom proteins, Tom5, Tom6, or Tom7.

The crosslinking patterns for the presequence of pSu9-DHFR between stage A and stage B can be compared. Because the cis site and trans site bound forms should differ in the interactions between the presequence of the fusion protein and the TOM complex, we expected different crosslinking patterns for the presequence between stage A and stage B. However, quite unexpectedly, the crosslinking patterns are nearly the same for residues 6, 11, and 15–29 in the presequence (Fig. 2*A*, lanes 1–12, and *B*). Not only the crosslinked partners such as Tom40 and Tom22 but also configurations of the crosslinked products do not differ significantly between stages A and B except for X5 involving Tom40.

On the other hand, the bands for the crosslinked products X4–X7 involving Tom40 and BPA at residue 108 in the mature DHFR domain are much stronger at stage B (bound at 30°C) (Fig. 2*A*, lane 16) than at stage A (bound at 0°C) (lane 14). The difference in crosslinking efficiencies of X4–X7 between stages A and B for positions 78, 88, 98, and 108 in the DHFR part can be seen in the quantification of the bands of the crosslinked products (Fig. 2*B*). These results shows that, although the relative and overall geometry between the presequence of the fusion protein and TOM proteins do not differ significantly between stages A and B, interactions between the DHFR domain of pSu9-DHFR and Tom40 is more enhanced at stage B than at stage A. Because the DHFR domain is unfolded only at stage B (Fig. 1), Tom40 may prefer the unfolded DHFR domain to the folded DHFR domain, thereby promoting the unfolding of the DHFR domain. This topology

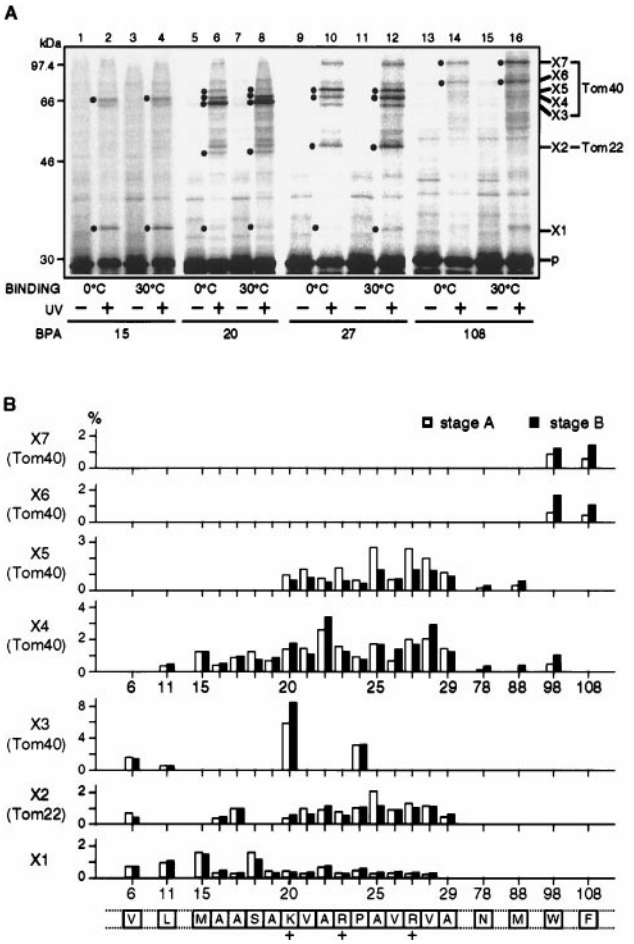

FIG. 2. Site-specific photocrosslinking reveals interactions between pSu9-DHFR and the TOM components at stages A and B. (*A*) pSu9-DHFR containing BPA at positions 15, 20, 27, and 108 was bound to CCCP-treated mitochondria for 10 min at 0°C (lanes 1, 2, 5, 6, 9, 10, 13, and 14) or at 30°C (lanes 3, 4, 7, 8, 11, 12, 15, and 16). The mitochondria were reisolated and suspended with MSC buffer containing 10 mM KCl. The samples were divided into halves. One aliquot was subjected to UV irradiation for 5 min at 0°C (even-numbered lanes). Proteins in all the samples were analyzed by SDS/PAGE. Dots indicate the crosslinked products X1–X7, the partners of which are identified as shown on the right side of the gel. Apparent molecular masses of X1, X2, X3, X4, X5, X6, and X7 are 34, 50, 65, 68, 74, 80, and 100 kDa, respectively, on a 10.5% gel, and those of X2, X3, X4, X5, X6, and X7 are 50, 65, 68, 70, 75, and 82 kDa, respectively, on an 8% gel. UV, UV irradiation; BPA, residues at which BPA was introduced; p, pSu9-DHFR. (*B*) Summary of the results of site-specific photocrosslinking. Crosslinking experiments were performed for the pSu9-DHFR translocation intermediate at stage A or stage B as described in *A*. The amounts of crosslinked products X1–X7 were quantified and plotted against the positions of introduced BPA (the boxes for the primary structure indicate the positions at which BPA was introduced). Open bars represent the stage A intermediate and solid bars represent the stage B intermediate. The amount of the precursor form of pSu9-DHFR recovered with mitochondria under the same conditions without UV irradiation was set to 100%.

of pSu9-DHFR at stage B may well make the MPP cleavage site partially inaccessible to externally added MPP.

The Presequence Is Already on the Trans Side of the Outer Membrane Both at Stage A and Stage B. Next, we asked where in the TOM complex the presequence of pSu9-DHFR is located at stages A and B. Thus, we compared the crosslinking patterns for the presequence of pSu9-DHFR between wild-type mitochondria with those for ΔC-Tom22 mitochondria (12) (Fig. 3). Deletion of the C-terminal IMS domain of Tom22 does not affect accumulation of the fusion protein at stages A or B (data not shown).

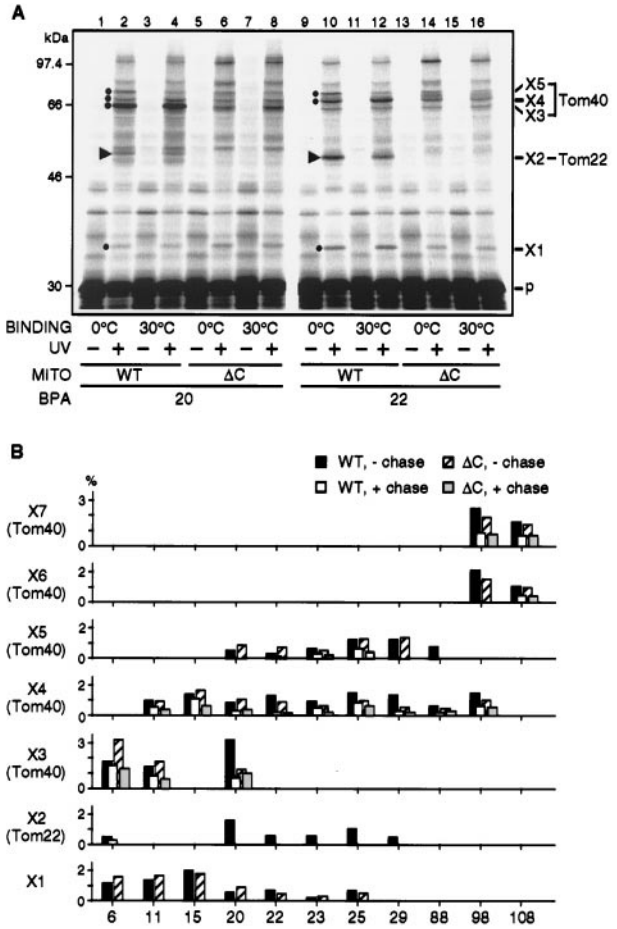

FIG. 3. Effects of deletion of the IMS domain of Tom22 on the crosslinking between pSu9-DHFR and the TOM components. (*A*) Mitochondria were prepared from the yeast MNMS-MAS17 strain (WT) or MNMS-MAS17Δ120–152 strain (ΔC). pSu9-DHFR containing BPA at position 20 or 22 was bound to CCCP-treated mitochondria at 0°C (lanes 1, 2, 5, 6, 9, 10, 13, and 14) or at 30°C (lanes 3, 4, 7, 8, 11, 12, 15, and 16). After binding, the mitochondria were isolated by centrifugation and subjected to UV irradiation for 5 min at 0°C (even-numbered lanes). UV, UV irradiation; MITO, mitochondria; BPA, positions at which BPA was introduced; p, pSu9-DHFR. Triangles indicate the crosslinked product X2 involving Tom22. Dots indicate the crosslinked products X1, X3, X4, and X5. (*B*) pSu9-DHFR containing BPA at positions 6, 11, 15, 20, 22, 23, 25, 29, 88, 98, and 108 was bound to CCCP-treated mitochondria prepared from MNMS-MAS17 (WT) or from MNMS-MAS17Δ120–152 (ΔC) at 30°C. The samples were diluted with MSC buffer containing 10 mM KCl and divided into halves, and the mitochondria were reisolated by centrifugation. One aliquot was resuspended with MSC buffer containing 10 mM KCl and kept on ice (− chase). The other aliquot was resuspended with chase buffer and incubated for 10 min at 30°C (+ chase). The samples were divided into halves and one aliquot was subjected to UV irradiation for 5 min at 0°C. Proteins in all samples were analyzed by SDS/PAGE, and yields of crosslinked products X1–X7 were quantified as described in Fig. 2.

The crosslinked product X2, which involves Tom22 and BPA at residues 20 and 22, with wild-type mitochondria (Fig. 3*A*, lanes 2, 4, 10, and 12) disappeared, with mitochondria bearing ΔC-Tom22 (Fig. 3*A*, lanes 6, 8, 14, and 16) for stages A and B. As a result, no crosslinked product was immunoprecipitated with anti-Tom22 antibodies for ΔC-Tom22 mitochondria. The crosslinking patterns for BPA at residues 6, 11, 15, 20, 22, 23, 25, 29, 88, 98, and 108 at stage B were quantified and compared between wild-type mitochondria and ΔC-Tom22 mitochondria (Fig. 3*B*, WT, − chase and ΔC, − chase). X2 involving BPA at residues 20, 22, 23, 25, and 29 observed with wild-type mitochondria (WT, − chase) disappeared with ΔC-Tom22 mitochondria (ΔC, − chase). Deletion of the Tom22 IMS domain did not significantly affect the rest of the crosslinking patterns except for X3 involving residues 6 and 20 of pSu9-DHFR. Similar results were obtained for stage A as well (not shown). Therefore, the presequence of pSu9-DHFR at stage A as well as at stage B is close to the IMS domain of Tom22. This indicates that even at stage A, the presequence of the fusion protein is already on the trans side of the outer membrane without concomitant unfolding of the DHFR domain. Therefore, the previous interpretation that unfolding of the mature DHFR domain of pSu9-DHFR is essential for the translocation of the presequence across the outer membrane (16) may be incorrect.

Chase from Stage B but Not from Stage A Takes Place at High Salt Concentrations but Requires the IMS Domain of Tom22. We next examined the effects of salt concentrations and deletion of the IMS domain of Tom22 on the stability of the productive translocation intermediates at stages A and B. The fusion protein was bound to wild-type mitochondria or those with ΔC-Tom22 at 0°C or at 30°C in low-salt (10 mM KCl) buffer and washed with buffers containing various concentrations of KCl. Subsequent reestablishment of $\Delta\Psi$ across the inner membrane by removal of CCCP allowed the bound fusion protein to be chased into the matrix; the fusion protein was processed and transported to a protease-protected location (Fig. 4). The efficiencies of the chase from both stages A and B were as much as 50% when wild-type mitochondria were

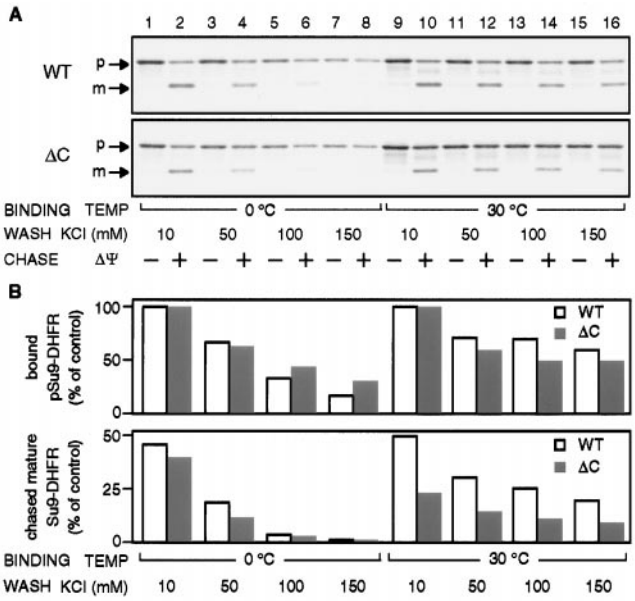

FIG. 4. Chase of pSu9-DHFR from stage B but not from stage A depends on the presence of the IMS domain of Tom22. (*A*) pSu9-DHFR was bound to CCCP-treated mitochondria prepared from MNMS-MAS17 (WT) or from MNMS-MAS17Δ120–152 (ΔC) at 0°C (lanes 1–8) or at 30°C (lanes 9–16). The samples were divided into four aliquots, which were diluted 5-fold with MSC buffer containing different concentrations of KCl to result in final KCl concentrations of 10 mM KCl (lanes 1, 2, 9, and 10), 50 mM KCl (lanes 3, 4, 11, and 12), 100 mM KCl (lanes 5, 6, 13, and 14), or 150 mM KCl (lanes 7, 8, 15, and 16) and incubated for 5 min at 0°C. The samples were divided into halves and the mitochondria were reisolated by centrifugation. One aliquot was resuspended with binding buffer and kept on ice (odd-numbered lanes). The other aliquot was resuspended with chase buffer and incubated for 10 min at 30°C (even-numbered lanes). p and m, precursor and mature forms of pSu9-DHFR, respectively. (*B Upper*) Quantification of the bound precursor form (odd-numbered lanes of *A*). (*Lower*) Chased mature-sized form (even-numbered lanes of *A*). The amount of the bound precursor form at 10 mM KCl at 0 or 30°C is set to 100%.

washed with low-salt (10 mM KCl) buffer (Fig. 4*B*). The chase from stage A (accumulated at 0°C) was sensitive to the salt concentration of washing buffer, and the efficiency of the chase with a prior wash at 100 mM KCl was 7% of that with a prior wash at 10 mM KCl (Fig. 4*B Lower*, 0°C, open bars). On the other hand, the chase from stage B (accumulated at 30°C) showed only moderate dependence on the salt concentration of washing buffer, and the efficiency of the chase with a prior wash at 100 mM KCl was 50% of that with a prior wash at 10 mM KCl (Fig. 4*B*, 30°C, solid bars). The difference in the salt sensitivity of the chased fractions between stages A and B is at least partly a result of a different stability of the intermediates accumulated at stage A and stage B, because the amount of the stage A intermediate decreased more significantly than that of the stage B intermediate as the salt concentration of washing buffer was increased (Fig. 4*B Upper*, open bars). These results suggest that the presequence binds to the TOM complex mainly through electrostatic interactions whereas the unfolded mature DHFR domain binds to the TOM complex at stage B through hydrophobic interactions as well as electrostatic ones. It is also to be noted that, although the stability of the stage A and stage B intermediates differs in their salt sensitivity in the washing step, their accumulation at both stage A and stage B depends significantly on salt concentrations in the binding step (data not shown), indicating that a salt-sensitive step(s) precedes both stage A and stage B.

When mitochondria with ΔC-Tom22 were used instead of wild-type mitochondria, the efficiency of the chase from stage B but not from stage A was reduced significantly; the fractions chased from stage B in ΔC-Tom22 mitochondria were about 50% of those in wild-type mitochondria (Fig. 4*B Lower*, open and solid bars). Although time-course experiments for the chase from stage B revealed that the amount of the chased fractions had already reached a plateau in the presence or absence of the Tom22 IMS domain within 10 min of the chase reaction (not shown), the decrease in the chase efficiency by deletion of the Tom22 IMS domain apparently is not a result of reduction of the stability of pSu9-DHFR accumulated at stage B (Fig. 4*B Upper*, solid bars). The chase from stage B with ΔC-Tom22 mitochondria still showed moderate dependence on the salt concentration of washing buffer as with wild-type mitochondria (Fig. 4*B Lower*, solid bars). The presence of the IMS domain of Tom 22 therefore is important, although not essential, for the chase, but not for the stability, of the stage B intermediate.

The IMS Domain of Tom22 Is Required for the Step That Is Later than Dissociation from TOM Proteins in the Chase of the Stage B Intermediate. The IMS domain of Tom22 appears to be important for the chase of the translocation intermediate of pSu9-DHFR from stage B into the matrix. A possible role of the Tom22 IMS domain in the efficient chase of the stage B intermediate might be that the Tom22 IMS domain allows pSu9-DHFR at stage B to interact with the TOM complex in such a way that is suitable for a subsequent chase reaction. However, this does not seem likely because deletion of the Tom22 IMS does not affect significantly the crosslinking pattern for BPA throughout the pSu9-DHFR polypeptide chain except for residue 20 (Fig. 3*B*).

Another possibility might be that the IMS domain of Tom 22 promotes dissociation of the fusion protein at stage B from the TOM complex, which allows subsequent translocation across the inner membrane. However, this possibility also seems unlikely for two reasons. First, for both wild-type mitochondria and those with ΔC-Tom22, the amounts of the crosslinked products were reduced significantly after reestablishment of ΔΨ (Fig. 3*B*, WT, + chase and ΔC, + chase), reflecting efficient dissociation of the fusion protein from the TOM complex at stage B irrespective of the presence of the Tom22 IMS domain. Second, there is an equilibrium between stages A and B, because the stage A intermediate was shifted to stage B by elevating temperature without regeneration of ΔΨ, and, conversely, the stage B intermediate was shifted to stage A by stabilizing the folded conformation of the DHFR domain by adding methotrexate/NADPH without regenerating ΔΨ (data not shown). However, the shift of the intermediate from stage B to stage A, which requires dissociation of the DHFR part from Tom 40, was not affected at all by deletion of the IMS domain of TOM 22 (data not shown).

We tried to follow the fate of the unprocessed, off-pathway form of pSu9-DHFR after regeneration of ΔΨ. pSu9-DHFR, which was off of the correct chase pathway was recovered with mitochondria after centrifugation, and its mature DHFR domain was digested by low concentrations of externally added protease (data not shown). This result suggests that, after dissociation from the TOM complex lacking the Tom22 IMS domain, a substantial fraction of pSu9-DHFR failed to interact with the TIM complex, yet remained bound to the mitochondrial surface. The IMS domain of Tom22 therefore is important, although not essential, for efficient transfer of the stage B intermediate from the TOM complex to the TIM translocation system in the presence of ΔΨ. The IMS domain of Tom22 perhaps may interact directly with the TIM proteins including the IMS domain of Tim23.

A New Model for Protein Translocation Across the Outer Membrane. The results described above suggest that the current model for protein translocation across the outer membrane, in which the presequence first binds to the cis and then to the trans site of the TOM complex and this presequence transfer is coupled to unfolding of the mature part of the precursor protein (16–18), should be reconsidered in the following respects. First, it is now clear that the presequence of pSu9-DHFR has already crossed the outer membrane at both stages A and B, but that the DHFR moiety of the fusion protein is unfolded and bound to Tom40 only at stage B (Fig. 2). Therefore, translocation of the presequence across the outer membrane and unfolding of the mature DHFR part are not coupled.

Second, although the presequence of pSu9-DHFR at both stage A and stage B is in the vicinity of the IMS domain of Tom22, the IMS domain of Tom22 is not essential for the stable interactions of the fusion protein with the TOM complex (Fig. 4*B*). In addition, the targeting signal region of the presequence and the mature DHFR domain interact with probably the same regions of Tom40 to generate the same crosslinked products X4 and X5 (Fig. 2*B*). These results may cast doubt on the presence of the trans site, which is proposed to be a well defined site on the trans side of the TOM complex for specific binding to the presequence (16).

Third, because the presequence of pSu9-DHFR accumulated at both stage A (previously assigned to the cis site-binding step) and stage B (previously assigned to the trans site-binding step) already has passed the outer membrane, there is no reason to assume a sequential model of the protein import in which stage B is placed downstream of stage A along the import pathway. Rather, the sequential model is not compatible with our present observation that the efficiency of the chase of the intermediate from stage B is reduced by deletion of the Tom22 IMS domain to about 50% of that with wild-type mitochondria whereas that from stage A is not affected by the Tom22 truncation.

Thus, we propose a new model in which stage A and stage B are placed in parallel along the import pathway from the cytosol to IMS (Fig. 5). Now, what is the significance of stage B in the import of precursor proteins? Because transfer of the intermediate at stage B but not at stage A from the TOM complex to the TIM system is promoted by the IMS domain of Tom22, the effects of deletion of the IMS domain of Tom22 on the import of pSu9-DHFR can be used to estimate the contribution of stage B to the entire import process. *In vitro* import of pSu9-DHFR into mitochondria is reduced moder-

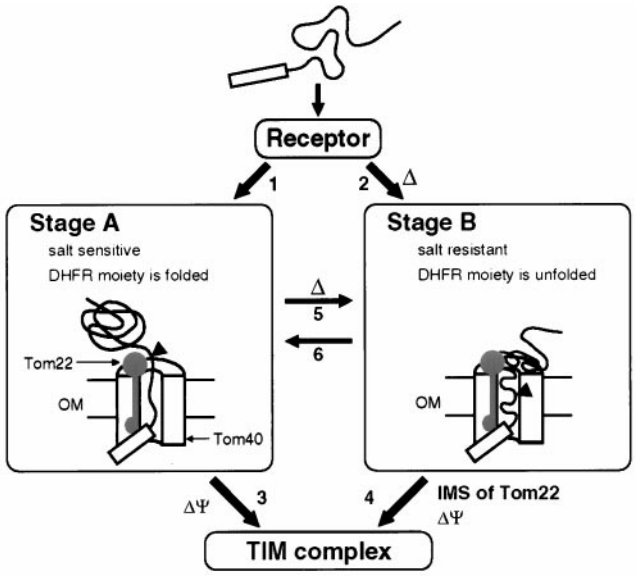

FIG. 5. A working model for protein translocation across the outer mitochondrial membrane. The triangle indicates the MPP cleavage site of the fusion protein. Δ, High temperature; IMS, the intermembrane space domain; 22, Tom22; 40, Tom40.

ately by about ≤30% by deletion of the IMS domain of Tom22 (12–14). Because efficiency of the chase of the pSu9-DHFR intermediate from stage B was reduced to 50% by deletion of the IMS domain of Tom22, we could estimate that, at most, one-half of the pSu9-DHFR molecules are imported into the matrix via stage B (through step 4 in Fig. 5). During the import of pSu9-DHFR into the matrix, transfer of the presequence from the TOM complex to the TIM complex likely takes place partly before a slow unfolding of the DHFR domain is completed. Then, interactions of the presequence of pSu9-DHFR with the TIM complex and Ssc1p, a mitochondrial hsp70, will drive further movement of the translocating polypeptide, and a fraction of the pSu9-DHFR molecules escapes stable interactions of the unfolded DHFR domain with Tom40 so that stage B is bypassed. Unfolding of the DHFR domain of the rest of the pSu9-DHFR molecules likely takes place before transfer of the presequence from the TOM complex to the TIM complex so that one-half of the pSu9-DHFR molecules are transiently populated at stage B, where the unfolded DHFR domain is stabilized by Tom40. All the pSu9-DHFR molecules are accumulated at stage B only under artificial conditions in which translocation across the inner membrane is blocked by dissipation of $\Delta\Psi$ at high temperature. The efficient import (≈50%) via stage A bypassing stage B again supports our conclusion that translocation of the presequence across the outer membrane and unfolding of the mature domain of the fusion protein are not necessarily coupled.

Although we have studied here the two distinct stages, stage A and stage B, only for the fusion protein pSu9-DHFR, the effects of deletion of the IMS domain of Tom22 were studied previously for various precursor proteins (11–14). The results from the three laboratories (12–14) agree well on the observation that deletion of the IMS domain of Tom22 reduced the import of precursor proteins by 0–30%. This suggests that, at most, one-half of the precursor protein molecules may be imported into mitochondrial via stage B depending on the length of the presequence, stability of the mature domain, and other factors.

We are grateful to Drs. S. Kitada and A. Ito (Kyushu University) for recombinant yeast MPP. This study was supported by a grant for the Biodesign Research Program from the Institute of Physical and Chemical Research (RIKEN), by Grants-in-aid for Scientific Research from the Ministry of Education, Science, and Culture of Japan, by a grant for the Research for the Future Program from JSPS, and by grants from Toray Science Foundation, Daiko Foundation, and CIBA–Geigy Foundation. P.G.S. is a Howard Hughes Medical Institute Investigator.

1. Omura, T. (1998) *J. Biochem.* **123,** 1010–1016.
2. Schatz, G. (1996) *J. Biol. Chem.* **271,** 31763–31766.
3. Neupert, W. (1997) *Annu. Rev. Biochem.* **66,** 863–917.
4. Pfanner, N., Craig, E. A. & Hölinger, A. (1997) *Annu. Rev. Cell Dev. Biol.* **13,** 25–51.
5. Endo, T. (1997) in *Molecular Chaperones in the Life Cycle of Proteins*, eds. Fink, A. L. & Goto, Y. (Dekker, New York), pp. 435–466.
6. Baker, K. P., Schaniel, A., Vestweber, D. & Schatz, G. (1990) *Nature (London)* **348,** 605–609.
7. Lithgow, T., Junne, T., Suda, K., Gratzer, S. & Schatz, G. (1994) *Proc. Natl. Acad. Sci. USA* **91,** 11973–11977.
8. Nakai, M. & Endo, T. (1995) *FEBS Lett.* **357,** 202–206.
9. Künkele, K.-P., Heins, S., Dembowski, M., Nargang, F. E., Benz, R., Thieffry, M., Walz, J., Lill, R., Nussberger, S. & Neupert, W. (1998) *Cell* **93,** 1009–1019.
10. Hill, K., Model, K., Ryan, M. T., Dietmeier, K., Martin, F., Wagner, R. & Pfanner, K. (1998) *Nature (London)* **395,** 516–521.
11. Bolliger, L., Junne, T., Schatz, G. & Lithgow, T. (1995) *EMBO J.* **14,** 6318–6326.
12. Nakai, M., Kinoshita, K. & Endo, T. (1995) *J. Biol. Chem.* **270,** 30571–30575.
13. Court, D. A., Nargang, F. E., Steiner, H., Hodges, R. S., Neupert, W. & Lill, R. (1996) *Mol. Cell Biol.* **16,** 4035–4042.
14. Moczko, M., Bömer, U., Kübrich, M., Zufall, N., Hönliger, A. & Pfanner, N. (1997) *Mol. Cell. Biol.* **17,** 6574–6584.
15. Nargang, F. E., Rapoport, D., Ritzel, G., Neupert, W. & Lill, R. (1998) *Mol. Cell. Biol.* **18,** 3173–3181.
16. Mayer, A., Neupert, W. & Lill, R. (1995) *Cell* **80,** 127–137.
17. Rapoport, D., Neupert, W. & Lill, R. (1997) *J. Biol. Chem.* **272,** 18725–18731.
18. Rapoport, D., Mayers, A., Neupert, W. & Lill, R. (1998) *J. Biol. Chem.* **273,** 8806–8813.
19. Kanamori, T., Nishikawa, S., Shin, I., Schultz, P. G. & Endo, T. (1997) *Proc. Natl. Acad. Sci. USA* **94,** 485–490.
20. Hurt, E., Pesold-Hurt, B. & Schatz, G. (1984) *EMBO J.* **3,** 3149–3156.
21. Kunkel, T. A., Roberts, J. D. & Zakour, R. A. (1987) *Methods Enzymol.* **154,** 367–382.
22. Daum, G., Böhni, P. C. & Schatz, G. (1982) *J. Biol. Chem.* **257,** 13028–13033.
23. Shimokata, K., Kitada, S., Ogishima, T. & Ito, A. (1998) *J. Biol. Chem.* **273,** 25158–25163.